2009

# Cell cycle checkpoint defects contribute to genomic instability in PTEN deficient cells independent of DNA DSB repair

Arun Gupta
*Washington University School of Medicine in St. Louis*

Qin Yang
*Washington University School of Medicine in St. Louis*

Raj K. Pandita
*Washington University School of Medicine in St. Louis*

Clayton R. Hunt
*Washington University School of Medicine in St. Louis*

Tao Xiang
*Washington University School of Medicine in St. Louis*

*See next page for additional authors*

[Cell Cycle 8:14, 2198-2210; 15 July 2009]; ©2009 Landes Bioscience

Report

# Cell cycle checkpoint defects contribute to genomic instability in PTEN deficient cells independent of DNA DSB repair

Arun Gupta,[1] Qin Yang,[1] Raj K. Pandita,[1] Clayton R. Hunt,[1] Tao Xiang,[1] Sandeep Misri,[1] Sicong Zeng,[1] Julia Pagan,[2] Jessie Jeffery,[2] Janusz Puc,[3] Rakesh Kumar,[1] Zhihui Feng,[1] Simon N. Powell,[1] Audesh Bhat,[1] Tomoko Yaguchi,[4] Renu Wadhwa,[4] Sunil C. Kaul,[4] Ramon Parsons,[3] Kum Kum Khanna[2] and Tej K. Pandita[1,*]

[1]Washington University School of Medicine; St. Louis, MO USA; [2]Queensland Institute of Medical Research; Brisbane, Queensland Australia; [3]Institute of Genetics; Columbia University; New York, NY USA; [4]National Institute of Advanced Industrial Science & Technology; Tsukuba, Ibaraki Japan.

**Key words:** genomic instability, checkpoint defects, DNA damage response, ATM, PTEN, Rad51

**Chromosomes in PTEN deficient cells display both numerical as well as structural alterations including regional amplification. We found that PTEN deficient cells displayed a normal DNA damage response (DDR) as evidenced by the ionizing radiation (IR)-induced phosphorylation of Ataxia Telangiectasia Mutated (ATM) as well as its effectors. PTEN deficient cells also had no defect in Rad51 expression or DNA damage repair kinetics post irradiation. In contrast, caffeine treatment specifically increased IR-induced chromosome aberrations and mitotic index only in cells with PTEN, and not in cells deficient for PTEN, suggesting that their checkpoints were defective. Furthermore, PTEN-deficient cells were unable to maintain active spindle checkpoint after taxol treatment. Genomic instability in PTEN deficient cells could not be attributed to lack of PTEN at centromeres, since no interaction was detected between centromeric DNA and PTEN in wild type cells. These results indicate that PTEN deficiency alters multiple cell cycle checkpoints possibly leaving less time for DNA damage repair and/or chromosome segregation as evidenced by the increased structural as well as numerical alterations seen in PTEN deficient cells.**

## Introduction

The PTEN (phosphatase and tensin homolog deleted on chromosome 10) gene encodes a major plasma membrane lipid phosphatase that functions in the phosphoinositide 3-kinase (PI3-K) signaling cascade and is often lost in various human cancers. Since loss of PTEN leads to PI3-K/AKT cascade activation as well as stimulating cell growth and proliferation,[1,2] this suggests loss of PTEN alters cell cycle kinetics due to cell cycle checkpoints failure. However, additional evidence is suggestive of other PTEN functions that are unrelated to PI3-K/AKT signaling.

The genomic instability observed in most cancers could be due to impairment of DNA damage checkpoint pathways or defective DNA damage repair or a combination of both. DNA double-strand breaks (DSBs) lead to chromosomal fragmentation and genomic rearrangements if not repaired in an accurate and timely manner. In mammalian cells, DSBs trigger a signaling response from the ATM pathway, initiating the nonhomologous end joining (NHEJ) or homologous recombination (HR) repair mechanisms. Cells deficient in PTEN function have been reported to have frequent structural as well as numerical chromosome alterations. Whether the chromosomal aberrations observed in PTEN deficient cells are due to defective pathways of DNA DSB repair is not clear. Previously we reported that *Pten*$^{-/-}$ mouse cells display a partially defective checkpoint in response to IR exposure due to lack of dephosphorylation of CHK1 at serine 280.[3] Primary breast carcinomas lacking PTEN expression have elevated AKT phosphorylation, increased cytoplasmic CHK1 and chromosomal aberrations.[3] We also reported that loss of PTEN and subsequent activation of AKT impairs CHK1 through phosphorylation, ubiquitination and reduced nuclear localization.[3] Consistent with the genomic instability phenotype in *Pten*$^{-/-}$ cells, Shen and coworkers reported that cells deficient in PTEN have defective DNA DSB repair, possibly due to lack of or down-regulation of Rad51 and lack of PTEN at centromeres.[4] Here we report that PTEN deficient cells express Rad51 and have a normal DNA damage response. However, PTEN deficiency not only eliminates S or $G_2$ checkpoints, but also eliminates the mitotic checkpoint response to spindle damage. We also did not observe an interaction between PTEN and centromeric proteins or DNA. Thus impairment of S and $G_2$-phase checkpoints as well as the mitotic checkpoint in PTEN deficient cells is the primary cause of the observed chromosomal aberrations including regional chromosome amplification.

*Correspondence to: Tej K. Pandita; Department of Radiation Oncology; Washington University School of Medicine; 4511 Forest Park Ave; St. Louis, MO 63108 USA; Tel.: 314.747.5461; Fax: 314.362.9790; Email: pandita@wustl.edu

Submitted: 05/06/09; Accepted: 05/07/09

Previously published online as a *Cell Cycle* E-publication: http://www.landesbioscience.com/journals/cc/article/8947

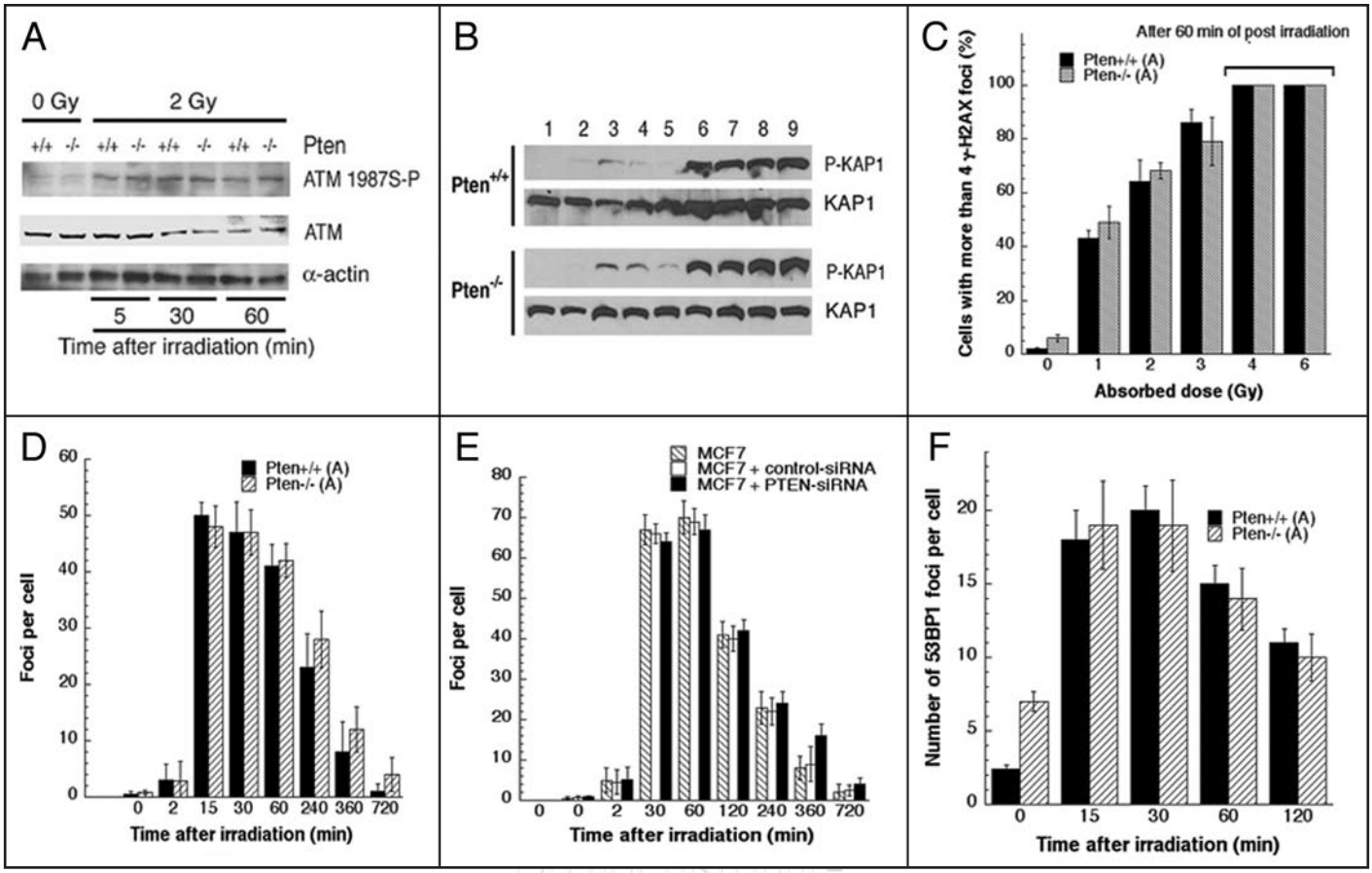


Figure 1. Effect of PTEN on ATM autophophorylation and its downstream effectors. (A) Exponentially growing MEF cells with and without PTEN were irradiated with 2 Gy and examined for ATM 1987S-P using specific antibody by western blot analysis. (B) MEFs were either heated at 43°C or irradiated with 2 Gy or heated first and then irradiated with 2 Gy and then examined at different periods of treatment for and KAP1 phosphorylation using specific antibody by western blot analysis. Lane 1: control; lane 2: heat shock for 30 min; lane 3: heat shock for 60 min; lane 4: heat shock for 30 min and recovery for 30 min at 37°C; lane 5: heat shock for 30 min and recovery for 60 min; lane 6: irradiation and recovery for 5 min; lane 7: irradiation followed by recovery for 30 min; lane 8: irradiation followed by recovery for 60 min; and lane 9: heat shock for 30 min followed by irradiation with 2 Gy and then recovery for 30 min postirradiation. (C) MEFs with and without PTEN were irradiated with different doses of IR and examined for γ-H2AX foci after 60 min of post irradiation. (D) MEFs treated with 1 Gy and then examined for γ-H2AX foci at different periods of post irradiation. (E) MCF7 cells with and without reduced levels of PTEN after 52 h of transfection with PTEN-siRNA were treated with 1 Gy and then examined for γ-H2AX foci at different periods of post irradiation. (F) MEFs treated with 1 Gy and then examined for 53BP1 foci at different periods of post irradiation.

## Results

**DNA damage response is independent of PTEN status.** Unstressed cells contain inactive ATM in a dimer or higher-order multimer form.[22] Several studies have suggested that chromatin alterations trigger rapid autophosphorylation of human ATM at Ser1981 (mouse Ser 1987), which causes dimer dissociation and initiates cellular ATM kinase activity.[7,22] Recent studies have suggested that PTEN is associated with chromatin and that loss of PTEN results in decreased Rad51 expression and genomic instability. Since alterations in chromatin structure are associated with ATM activation, we determined whether cells with and without PTEN show any difference in spontaneous as well as IR-induced ATM autophosphorylation. No differences in spontaneous as well as IR-induced ATM activation was found between cells with and without PTEN, suggesting that PTEN does not have any effect on chromatin structure following irradiation that could influence DNA damage signaling (Fig. 1A). Although PTEN has no role in ATM activation, it is possible that PTEN may be important in the function of down stream repair proteins.

Based on the fact that PTEN deficient cells have higher genomic instability, it is possible that PTEN may modify chromatin structure and thus influence the repair of DNA DSB.[4] A direct connection between chromatin alteration and ATM was made when the transcriptional corepressor Kruppel-associated box (KRAB)-associated protein (KAP)-1 was identified as an ATM substrate, being robustly phosphorylated at S824 upon DNA damage and causing transient chromatin relaxation.[23] Since heat shock is known to induce chromatin alterations, a trigger to ATM autophosphorylation,[12] we determined the influence of PTEN on heat shock or IR-induced KAP-1 phosphorylation. Cells were either heated at 43°C for different periods or irradiated or first heated then irradiated and examined for KAP-1 phosphorylation. No difference in heat or IR or heat + IR induced KAP-1

phosphorylation was found between *Pten*$^{+/+}$ and *Pten*$^{-/-}$ MEF cells, suggesting that Pten has a minimal role in damage induced chromatin modifications (Fig. 1B). We further determined whether the heat shock response was intact in *Pten*$^{-/-}$ cells and found no difference in HSP70 response irrespective of PTEN status (Suppl. Fig. 1).

Although PTEN deficient cells show normal IR-induced ATM and KAP1 phosphorylation it is possible that PTEN inactivation may influence other DNA damage response (DDR) components that could account for the higher frequency of chromosomal aberrations observed in PTEN null cells.[3,4] One of the early events in the DDR is H2AX phosphorylation, which is associated with the formation of nuclear foci containing factors that are essential for DNA repair, replication and cell cycle regulation.[24-26] H2AX phosphorylation coincides with sites of DSBs, irrespective of their origin[27-31] and is critical for protecting the genome from spontaneous DSBs, as well as those induced by IR or V(D)J recombination.[32,33] We examined whether PTEN deficiency influenced the appearance of IR-induced γ-H2AX foci. Cells with and without PTEN treated with increasing doses of IR displayed similar frequency of cells with γ-H2AX foci (Fig. 1C). As reported previously,[4] PTEN deficient mouse cells have slightly higher base line γ-H2AX foci per cell as compared to control cells with PTEN (Fig. 1C). To determine whether there is a difference in the formation and disappearance of IR-induced γ-H2AX foci in PTEN null and wild type cells, exponentially growing cells were exposed to 1 Gy of IR and monitored for γ-H2AX foci formation/disappearance at various time points post irradiation (Fig. 1D). The kinetics of γ-H2AX foci appearance was almost identical in cells with and without PTEN. However, mouse as well as human PTEN deficient cells did show slightly higher residual γ-H2AX foci six hr post-irradiation (Fig. 1D and E). There are multiple possibilities for having higher residual γ-H2AX foci in PTEN deficient cells, e.g., (1) defective DNA DSB repair and/or (2) defective cell cycle checkpoints.

The 53BP1 protein becomes progressively, yet transiently, immobilized on chromatin adjacent to DSB within minutes of DNA damage[34] and is a major component of the genome surveillance network activated by DNA DSB. To test whether PTEN deficiency influences IR-induced 53BP1 foci formation, cells with and without PTEN were treated with 2 Gy and 53BP1 foci were detected by immunofluorescence (Fig. 1F). Again, while cells deficient for PTEN had higher basal level 53BP1 foci, irradiated cells with and without PTEN showed similar kinetics of 53BP1 foci appearance and disappearance.

**Rad51 levels and IR-induced Rad51 foci formation in cells with and without PTEN.** The role of PTEN's lipid phosphatase activity as a negative regulator of the cytoplasmic phosphatidylinositol-3-kinase (PI3K)/Akt pathway is well known. Recent studies support its role in regulating cellular pathways in other compartments of the cell, specifically in maintaining genomic stability through transcriptional regulation of RAD51.[4] It has been postulated that the increased genomic instability seen in PTEN-deficient cells is due to defective Rad51-mediated recombinational repair of DNA damage since Rad51 levels were shown to be markedly reduced in PTEN-deficient cells.[4] We found, however, that PTEN deficient cells did not show loss of Rad51 expression (Fig. 2A and Suppl. Fig. 2) and had normal IR-induced Rad51 foci formation (Fig. 2B). We did observe, however, that western blot detection of Rad51 in different cell types could be antibody dependent (see Fig. 2A, last 2 lanes). Based on these results, we next determined directly whether PTEN influences homology-directed repair. Repair was measured by examining the reconstitution frequency of a GFP reporter gene (pDR-GFP) within a chromosomally integrated plasmid substrate in MCF7 cells with normal or reduced levels of PTEN (Fig. 2C) as described previously.[5] Following I-SceI transfection to induce the site specific DSBs, both control and PTEN siRNA transfected cells containing the pDR-GFP substrate demonstrated a comparable increase (>80-fold) in the number of GFP-positive cells over cells without I-SecI transfection (Fig. 2D), providing evidence that PTEN deficiency does not affect the HR pathway for DNA DSB repair.

PTEN-deficient cells were frequently observed to have small chromatin fragments in the form of circular chromosomes as well as amplified chromosomal regions with multiple centromeres (Fig. 3A). Similar chromosomal aberrations have been linked with aberrant DNA amplification, which may or may not be due to defective DNA repair. To determine whether PTEN deficiency influences sister chromatid exchanges (SCEs), which occur during S-phase and correlate with recombinational repair specifically, cells with and without PTEN were examined for the frequency of SCEs observed at metaphase using the conventional fluorescent plus giemsa technique.[16] No significant difference in the frequency of SCEs was found between cells with and without PTEN (data not shown) reinforcing the notion that recombinational repair is not affected by loss of PTEN.

**Amplification of chromosome regions in Pten null cells.** Post DNA replication, the two telomeres at the end of a duplicated chromosome can recombine, which can be visualized in metaphase chromosomes by Chromosome Orientation Fluorescent In Situ Hybridization (CO-FISH) as described previously.[35] Telomere sister chromatid exchanges are an indication of relaxed control of DNA repair at telomeres but also constitute a potential threat to telomere function because unequal exchanges will elongate one sister telomere at the expense of another. Since PTEN deficient cells show amplified chromosome fragments with multiple telomere bands (Fig. 3A, part c), we first established whether telomere length is affected by inactivation of PTEN and found that there is a modest heterogeneity in telomere size in cells lacking PTEN (Suppl. Fig. 3). We then determined whether telomere amplification occurs due to chromosome region specific defective recombination. This was achieved by performing CO-FISH, which involves incorporation of BrdU/BrdC during one round of DNA replication, in order to destroy newly synthesized telomeric G- and C-rich strands by photolysis and exonuclease digestion. The parental strands were detected with differentially labeled probes for the C- and G-rich telomeric strands (Fig. 3A). PTEN deficiency did not result in telomere specific sister chromatid exchanges, indicating PTEN deficiency has no effect on telomere or global sister chromatid exchange repair processes.

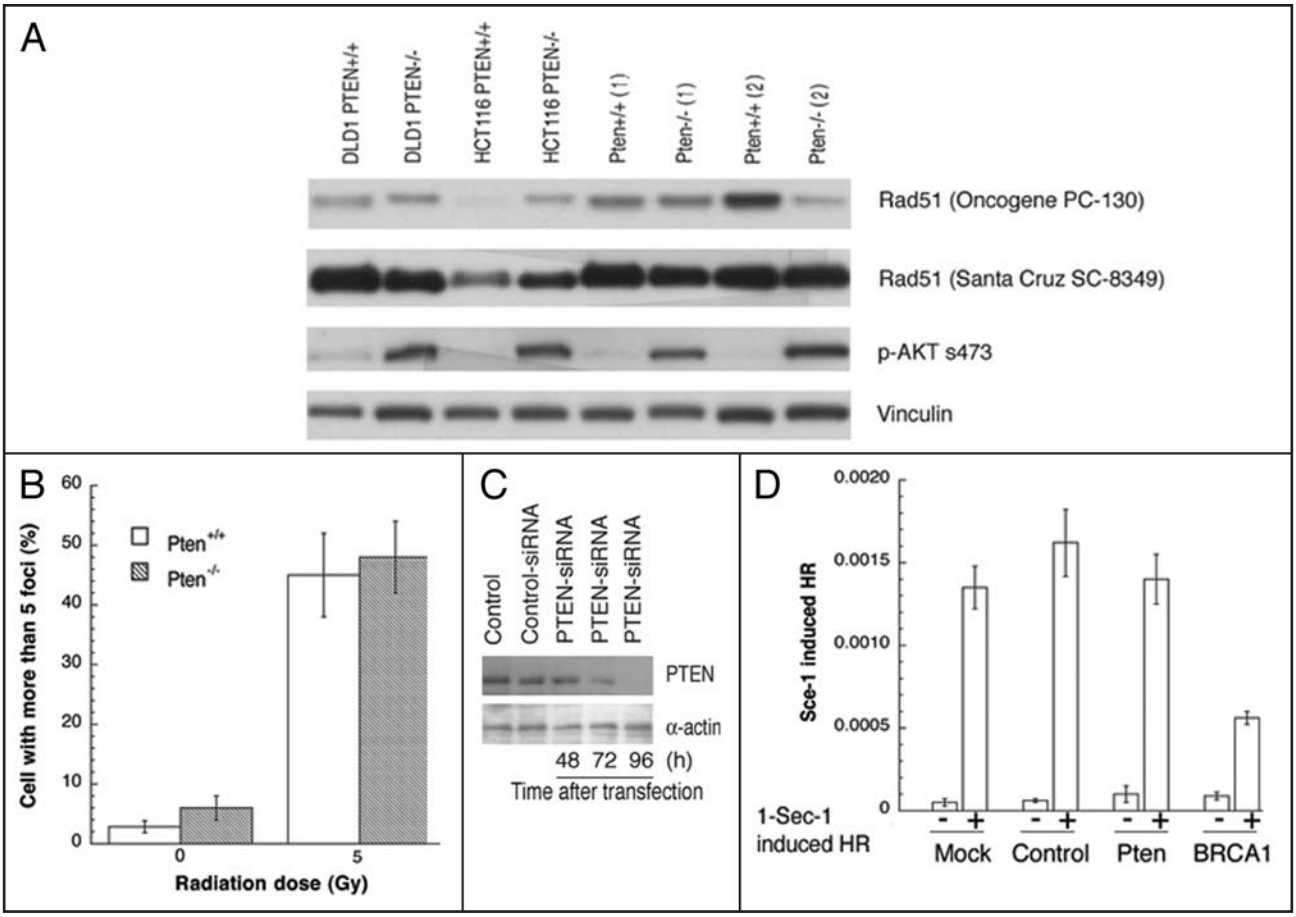


Figure 2. Rad51 expression and HR repair in cells with and without reduced PTEN levels. (A) Different human, MEF (*Pten* 1) and ES (*Pten* 2) cells with and without PTEN were examined for Rad51 expression by western blot using anti-Rad51 antibody from different sources. PTEN deficient cells have constitutively activated AKT as determined by the phosphorylation status using p-AKT s473 specific antibody. (B) MEFs with and without PTEN were irradiated with 5 Gy and examined for Rad51 foci after three hr of post irradiation. (C) Knockdown of PTEN by PTEN specific siRNA in MCF7 cells. (D) PTEN knockdown does not influences HR. Normal I-SceI-induced HR in PTEN-deficient MCF-7 cells was found. HR was measured by dual-color flow cytometric detection of GFP-positive cells. HR frequencies are shown with (+) or without (-) I-SceI induction for untreated cells, for cells treated with control siRNA, and for cells treated with PTEN-specific siRNA. PTEN-deficient cells did not show reductions in HR. The knockdown of BRCA1 by BRCA1 siRNA in MCF-7 cells has been described previously.[5] The results presented are the mean and standard error from three independent experiments.

PTEN deficient cells also contained chromosome fragments with multiple centromeres (Fig. 3A, part c), that lacked detectable telomeric signals. These structures can be the result of abnormal DNA replication, which can result in the development of chromosome fragments with either single or multiple centromeres as observed in PTEN deficient cells. The CO-FISH studies, however, did not suggest any aberrant telomere specific sister chromatid exchanges (Fig. 3A, parts e–i), supporting the argument that homology directed repair is intact in PTEN deficient cells. Since CO-FISH has limited sensitivity for detecting telomere specific sister chromatid exchanges, a biochemical assay was utilized to determine if there are any differences in homology directed repair between cells with and without PTEN.

Homologous recombination activity at the telomeres was determined by analyzing T-loop-sized circular DNAs in cells with and without PTEN. This was achieved by analyzing telomeric DNA using neutral-neutral 2D gel electrophoresis, which separates telomeric restriction fragments first by size and then by shape.[20,21] Cells with and without PTEN did not display any new arc of telomeric DNA as did cells used as positive control, which produced a new arc of telomeric DNA, whose migration was consistent with that of relaxed, double-stranded circles (Fig. 3B). The absence of arcs in cells with and without PTEN suggests that lack of PTEN does not alter HR repair even at the telomeric regions.

Mouse cells deficient for PTEN show frequent breaks near centromere regions that have been attributed to the absence of PTEN in the centromere regions.[4] PTEN deficient cells also show frequent chromosome fragments with and without amplified centromeres. We analyzed by immunostaining whether PTEN colocalizes with the centromere protein CENPC using various PTEN antibodies available from different sources and could not detect nuclear PTEN in most normal cells (Fig. 4A). This staining was specific as signal was abolished in PTEN-deficient cells. However, upon DNA damage, PTEN was found to show some nuclear staining, however, CENPC, as expected, was always found in the nucleus of both primary as well as immortalized cell

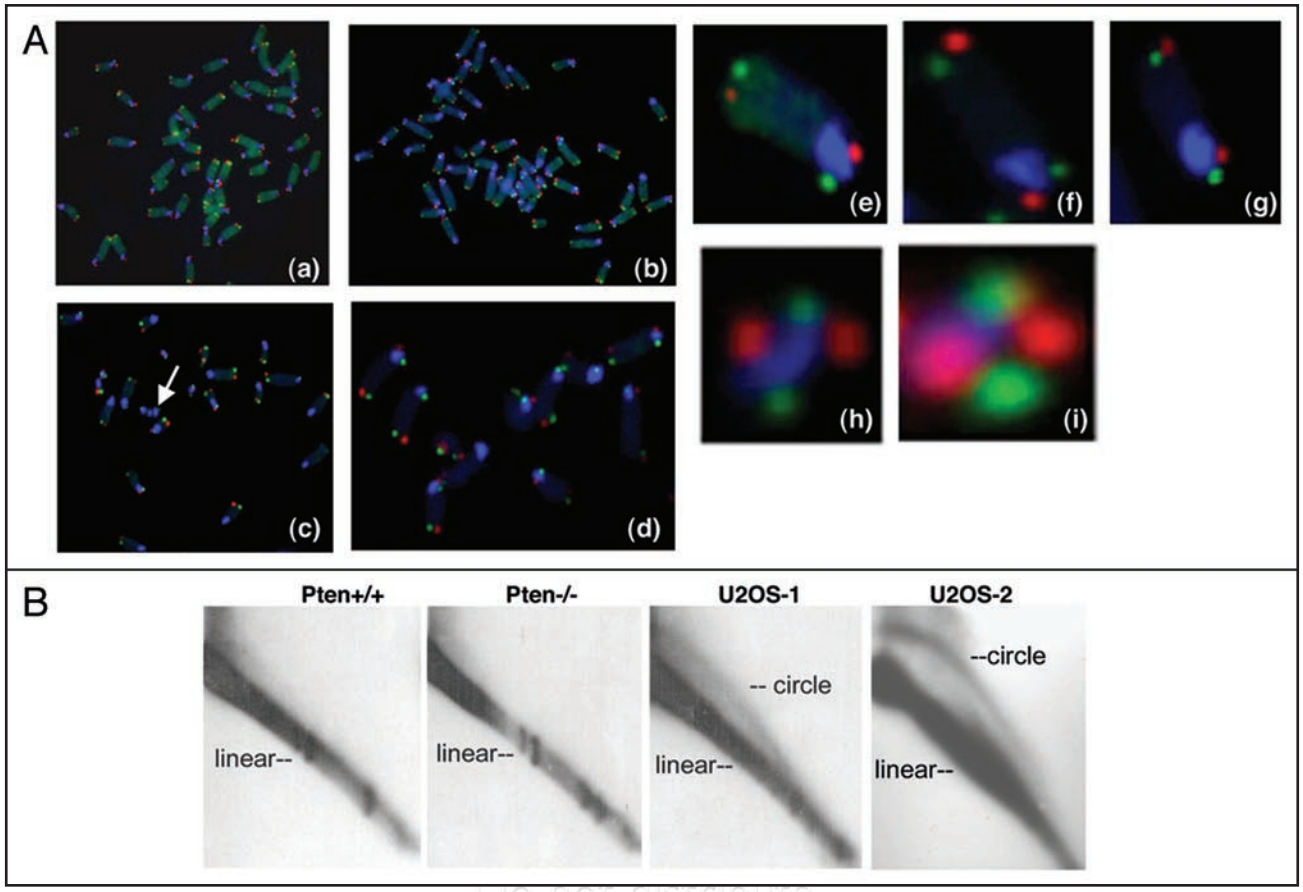




Figure 3. PTEN deficient MEF cells have normal recombination at the telomeres. (A) Telomere strand specific orientation analysis at metaphase. Cells with (Part a) and without (Part b) PTEN showing strand specific telomere FISH performed as described in the material and methods. PTEN deficient have amplified chromosome regions as indicated by the arrow (Part c) and chromosome fragments (Part d). The opposite orientation of the telomere strands FISH of the large chromosomes of cells with (Part e) and without PTEN (Part f), however opposite to this orientation (Part g) was observed in cells with and without PTEN. Small chromosomes also showed similar orientation of telomere stands in cells with (Part h) and without (Part i) PTEN as detected at high magnification. (B) Pten-deficiency does not induce telomeric circles. Genomic DNA from $Pten^{+/+}$ or $Pten^{-/-}$ MEFs was separated by size (1D) and then shape (2D), blotted, and probed for telomeric DNA. Circular telomeric DNA was not detected in these cells. U2OS cells (ALT cells) were as a positive control. The 2D gels showed the elevated levels of circular telomeric DNA from U2OS cells.

lines (Fig. 4B, data not shown). Furthermore, we analyzed the interaction of PTEN with centromeric DNA in human as well as mouse cells by chromatin immunoprecipitation and could not detect an interaction between centromeric DNA and PTEN (Fig. 4C and D), whereas CENPC was always found to interact with centromeric DNA, suggesting PTEN may have an indirect role in fragmentation of chromosomes near centromeres and/or subsequent centromeric amplification.

**DNA DSB repair kinetics in cells with and without PTEN.** The results described above do not support the idea that PTEN deficient cells have defective recombinational repair of DNA damage, however, the increased genomic instability seen in PTEN null cells could result from defective DNA end ligation. Most cells with DNA repair factor defects demonstrate slow repair kinetics and/or a higher level of residual DNA DSBs at 120 min post irradiation.[36,37] Therefore, we directly determined whether PTEN deficient cells exhibit increased levels of initial DNA DSBs compared to normal cells since this might be an important factor in determining cellular sensitivity.[38,39] Exponentially growing cells were prelabeled with [14C] dThd, irradiated with doses from 0 to 50 Gy, and analyzed immediately for DNA DSBs using the neutral DNA DSB assay. As shown in Figure 5A, *Pten*$^{-/-}$ cells showed similar levels of initial DNA damage to *Pten*$^{+/+}$ cells. Similar results were obtained when exponentially growing *Pten*$^{-/-}$ and *Pten*$^{+/+}$ MEF cells or MCF cells with reduced PTEN levels were irradiated with a dose of 20 Gy, and analyzed immediately for DNA DSBs by pulsed field gel electrophoresis (Fig. 5B and C). Thus, no effect of PTEN on IR-induced initial DNA damage was observed in multiple different assays. We further examined the influence of PTEN on DNA DSB repair after IR exposure. Cells were irradiated with 20 Gy and, allowed to repair for 90 min or 180 min before unrepaired DNA DSBs were measured by PFGE (Fig. 5B and C). No difference in residual DNA damage was observed at 90 min post irradiation in cells with and without PTEN. Similar results were observed when cells were enriched in $G_1$-, S- or $G_2$/M-phases of the cell cycle by centrifugal elutriation and DNA DSB repair measured for up to 120 min post-irradiation, suggesting PTEN does not play a role in DNA DSB repair (Fig. 5D). These

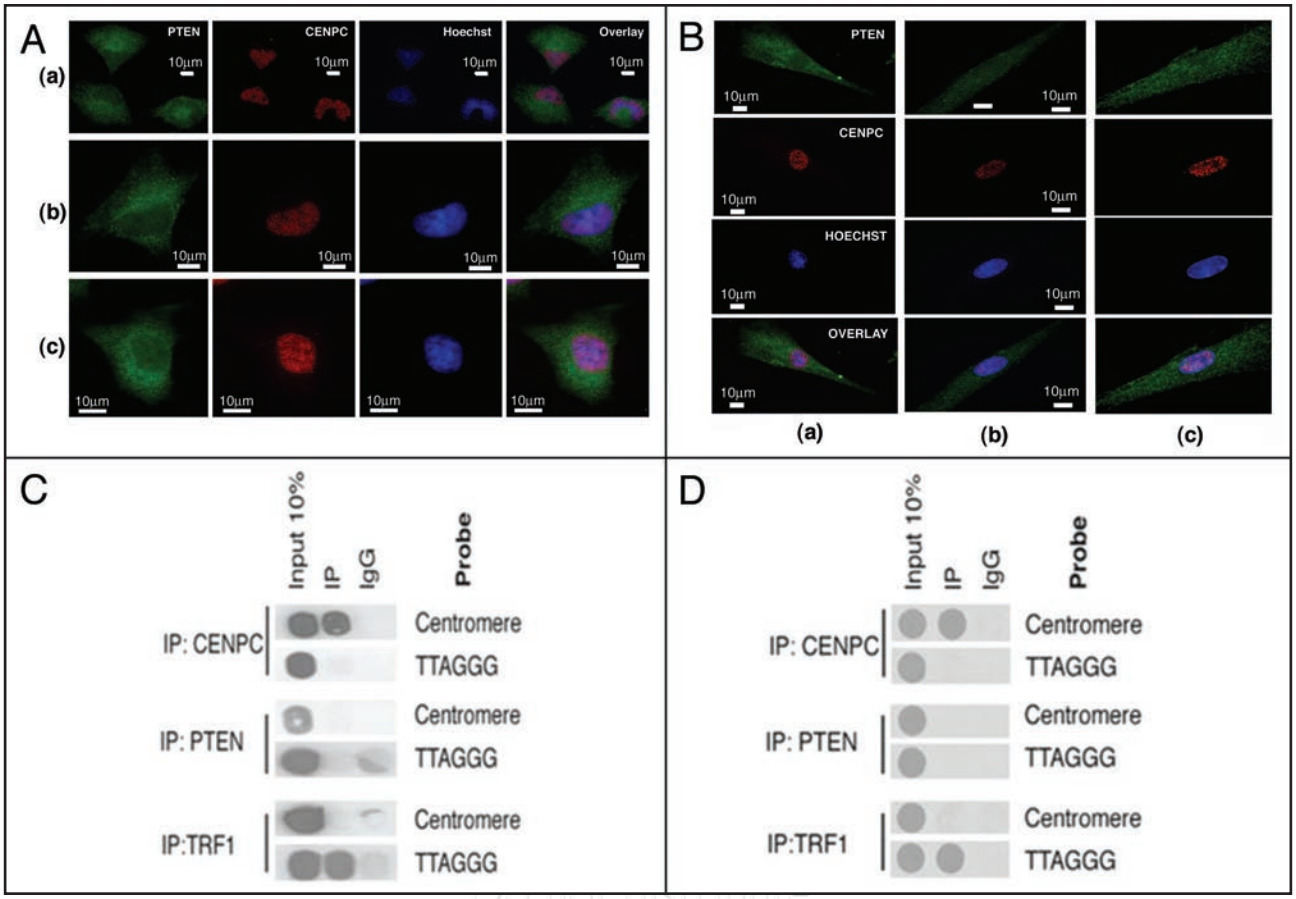


Figure 4. Localization and interaction of PTEN centromeric DNA. (A) PTEN and CENPC immunostaining in three different cell types (Parts A–C). (B) Cells were treated with hydrogen peroxide and examined for the PTEN and CENPC: (Part A) control, (Parts B and C) treated and examined for PTEN and CENPC after 1 h (Part B) and 6 h (Part C). (C and D) DNA coimmunoprecipitated by different antibodies (anti-TRF1, anti-CENPC and anti-PTEN) after in vivo cross-linking in human cells. Proteins were treated with formaldehyde [(C) represents immunoprecipitated DNA from mouse cells and (D) represents immunoprecipitated DNA from human MCF cell line]. Chromatin was isolated and subjected to immunoprecipitation by using an anti-TRF1 or anti-CENPC or PTEN antibody. Deproteinized DNA isolated from the precipitates was denatured and spotted onto a membrane. The following probes were used for hybridization: Total human genomic DNA (total DNA), centromeric DNA probe, or a DNA fragment containing telomeric DNA (CCCTAA). The same blot is shown after consecutive rehybridizations with the different probes. The results are representative of three independent experiments.

results do not support the model that the increased chromosomal aberrations observed in PTEN-deficient cells are due to a defective DNA DSB repair process. Although PTEN deficient cells did not display any difference in the repair kinetics or levels of residual DNA DSB, they did have a modest increase in post irradiation cell survival (Suppl. Fig. 4).

We next considered the possibility that the higher levels of chromosome aberrations observed in PTEN deficient cells at metaphase might be due to the loss of cell cycle checkpoints. One way to test this notion is to compare cell cycle stage-specific chromosomal aberrations in *Pten*$^{+/+}$ and *Pten*$^{-/-}$ cells. Cell cycle phase-specific chromosome aberrations were ascertained based on the frequency of chromosomal and chromatid-type aberrations observed at metaphase as described previously.[5] $G_1$-specific aberrations detected at metaphase are mostly of the chromosomal type (dicentric with acentric fragment), with a few involving chromatids. S-type aberrations detected at metaphase are both chromosome as well as chromatid type and $G_2$-type aberrations detected at metaphase are predominantly the chromatid type with the least number of dicentrics. To determine $G_1$-type chromosome damage, cells were treated with 3 Gy and replated 18 h after irradiation, and aberrations were scored at metaphase as previously described.[5,6] No difference in residual IR-induced $G_1$ chromosomal aberrations was seen in metaphase *Pten*$^{-/-}$ and *Pten*$^{+/+}$ cells (Fig. 6A, part a). To determine S-phase-specific chromosome aberrations, we first determined the time needed for S-phase cells to reach metaphase after IR exposure. Exponentially growing cells were labeled with BrdU for 30 min as previously described[5] and then irradiated with 2 Gy. Anti-BrdU immunostaining was performed to determine when metaphase chromosomes contained BrdU. In these experiments, BrdU-labeled metaphases appeared approximately 3 h post-irradiation (data not shown). The IR dose for analyzing S-phase specific aberrations was selected to produce a level similar to the $G_1$-type of chromosomal aberration induced by IR. Thus, *Pten*$^{-/-}$ and *Pten*$^{+/+}$ cells were treated with 2 Gy of IR and metaphases were collected 4 to 5 h post-irradiation. *Pten*$^{-/-}$ cells thus treated displayed higher frequencies of metaphases with chromatid and chromosomal aberrations after IR exposure compared to *Pten*$^{+/+}$ cells (Fig. 6B, part a).

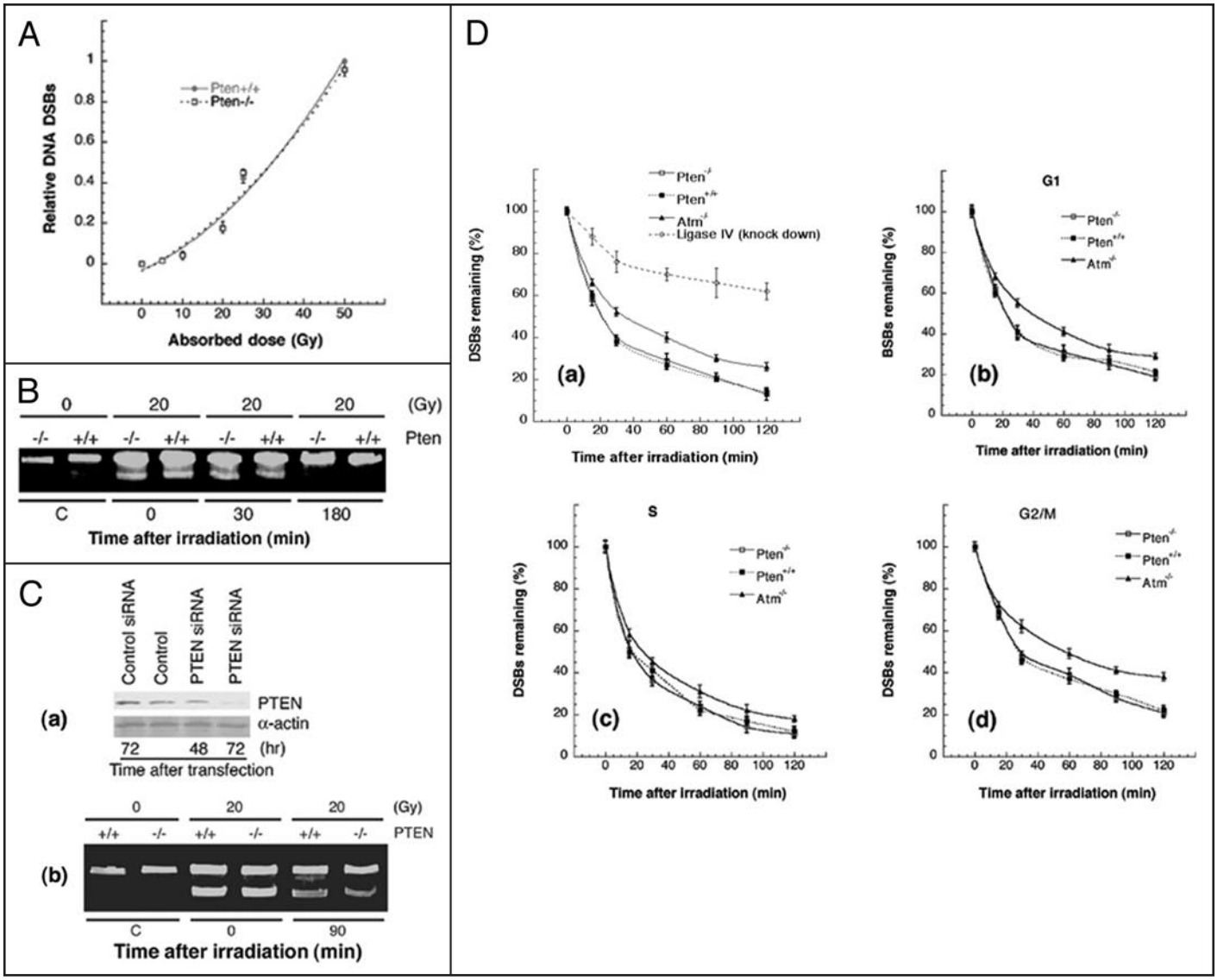


Figure 5. DNA DSB repair analysis. (A) Initial levels of DNA DSBs (relative elution) as a function of dose in MEFs with and without PTEN. (B and C) Initial DNA DSB and residual DSB examined by pulse field gel electrophoresis. MEFs with and without PTEN (B) and HeLa (C) cells with PTEN knockdown with specific siRNA (Part a) were irradiated with 20 Gy and incubated at 37°C for different periods post irradiation for repair and examined for residual DNA DSB. (D) The unrepaired DNA breaks after 20 Gy exposure were measured by neutral filter elution in MEFs with and without PTEN. Mouse cell without ATM or with knockdown of Ligase IV were used at positive control. (Part a) Asynchronous cells; (Part b) Enriched $G_1$-phase cells; (Part c) enriched S-phase cells and; (Part d) enriched $G_2$/M phase cells. The data represent the means of three independent experiments.

Furthermore, when cells were treated with 1 Gy of gamma rays and analyzed 1 h after to determine $G_2$-phase-specific chromatid aberrations, *Pten*$^{-/-}$ cells showed increased aberrations (Fig. 6C, part a). These observations suggest that PTEN inactivation results in a higher frequency of S- and $G_2$-specific chromosomal aberrations. Ectopic expression of PTEN in *Pten*$^{-/-}$ cells decreased the frequency of higher chromosome aberrations to levels similar to that of *Pten*$^{+/+}$ cells (Suppl. Fig. 5).

**Defective cell cycle checkpoints in PTEN null cells increases chromosomal aberrations.** To determine whether the increased cell cycle phase specific IR-induced chromosome aberrations in PTEN deficient cells are due to a cell cycle defect, we abrogated DNA damage induced cell cycle checkpoints by treating cells with caffeine, a pharmacological inhibitor of ATM/ATR and then analyzed IR-induced chromosome aberrations at metaphase at different time points post irradiation. Caffeine treatment or treatment with the ATM inhibitor (KU55933) did increase IR-induced $G_1$-type chromosome aberrations in both *Pten*$^{-/-}$ and *Pten*$^{+/+}$ cells (Fig. 6A, part b, and data not shown). However, caffeine or KU-55933 treatment only increased IR-induced S- and $G_2$-phase chromosome aberrations, as well as the mitotic index, in *Pten*$^{+/+}$ cells, whereas the *Pten*$^{-/-}$ cell response was unaltered (Fig. 6B, part b; C, part b; D, parts a and b; and data not shown). In addition, pharmacological inhibition of CHK1 (with Go6976) increased chromosomal aberrations only in *Pten*$^{+/+}$ cells (data not shown). Based on the fact that pharmacological inhibition

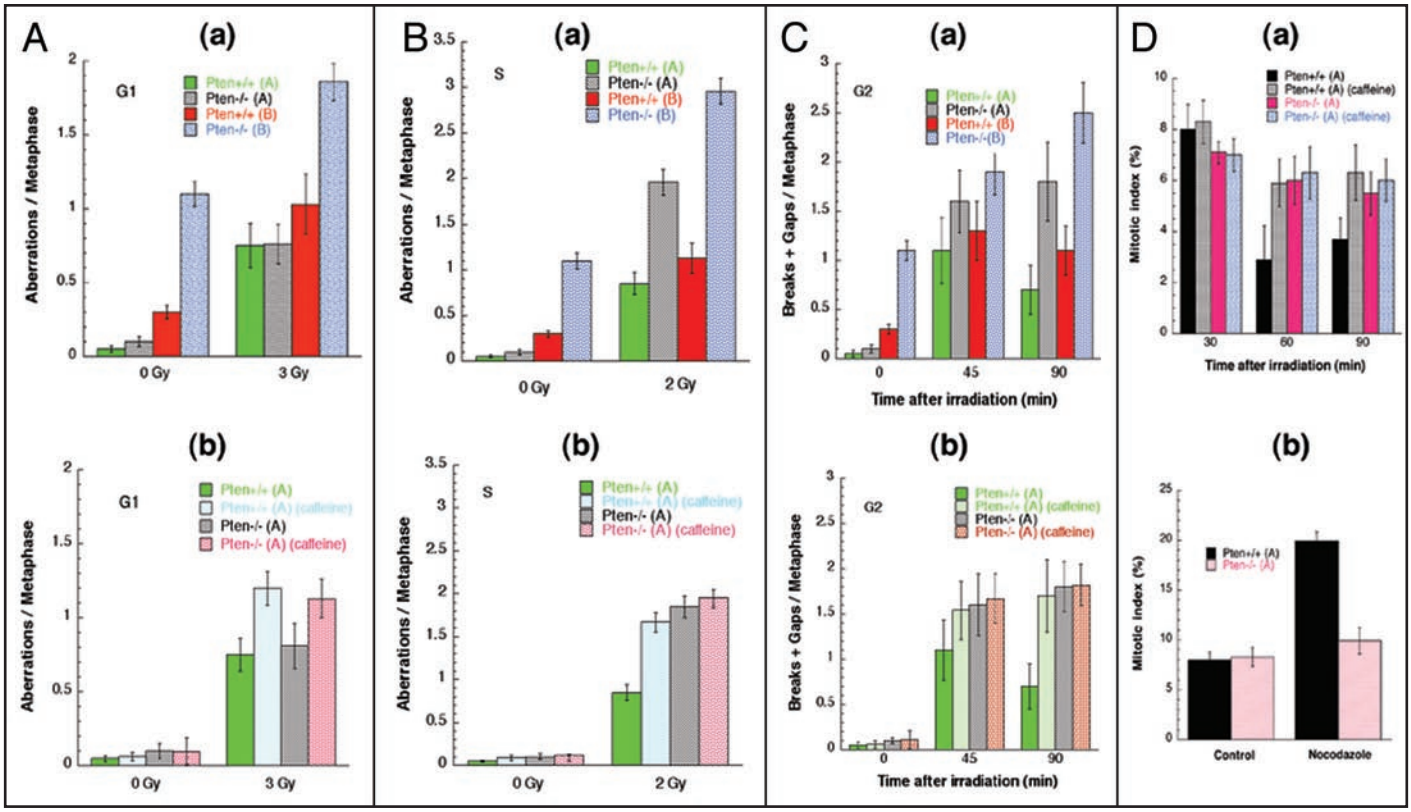




Figure 6. Effect of caffeine on the IR-induced $G_1$, S and $G_2$ chromosomal aberrations in cells with and without PTEN. Chromosomal aberrations after IR, or caffeine and IR treatment in mouse embryonic stem cells with and without Pten. (A) Cells were either irradiated with 3 Gy (Part a) or first treated with caffeine (Part b) and then irradiated, incubated for 14 h postirradiation, and then subcultured, and metaphases were collected. $G_1$-type aberrations were examined at metaphase. Categories of asymmetric chromosome aberrations scored included dicentrics, centric rings, interstitial deletions-acentric rings, and terminal deletions. (B) Cells were either irradiated with 2 Gy (Part a) or first treated with caffeine and then irradiation with 2 Gy. Metaphases were harvested after 3–4 h following irradiation and examined for chromosomal aberrations. (C) Cells were either irradiated with 1 Gy (Part a) or first treated with caffeine followed by irradiation with 1 Gy (Part b). Metaphases were harvested after 1 h following irradiation and examined for chromosomal aberrations. (D) Cells were treated with either with 1 Gy of γ rays (a) or first treated with caffeine followed by irradiation (b). Cells were harvested 30, 60 and 90 min later and examined for mitoses.

of ATM and ATR or CHK1 did not enhance S- and $G_2$-phase IR-induced chromosome aberration in *Pten*$^{-/-}$ cells, this suggests that such cells have abrogated S- as well as $G_2$-checkpoints. Next we determined whether a defect in IR-induced activation of the ATM/ATR pathway was responsible for defective S- and $G_2$-checkpoints in *Pten*$^{-/-}$ cells. Our results indicated that this was unlikely since ATM activation and activity as assessed by Ser 1981 autophosphorylation and phosphorylation of ATM targets, including KAP1 and SMC1, was unaltered (Fig. 1, Suppl. Fig. 7). In addition, the IR-induced recruitment of ATR and RPA to DSBs in S and $G_2$ cells, a measure of ATR activation and activity, was normal (data not shown). In contrast, damage-induced CHK1 phosphorylation on Ser317 was significantly impaired in *Pten*$^{-/-}$ cells, which is in line with a previous report that elevated AKT mediated phosphorylation of CHK1 on S280 antagonizes DNA damage-induced phosphorylation of CHK1 (Suppl. Fig. 7, reviewed in ref. 3). Overall these results do not support the notion that PTEN acts at the level of ATM and ATR to regulate genomic stability but rather confirm that the PTEN-AKT pathway regulates the CHK1 dependent checkpoint response and genomic stability.

**PTEN-deficient cells bypass Taxol-induced mitotic arrest.** Cells deficient for PTEN also exhibit numerical chromosomal alterations (polyploidy as well as aneuploidy; Suppl. Fig. 6). These alterations have not been attributed to defective S- or $G_2$-checkpoints but rather to a defective mitotic checkpoint,[40] suggesting that PTEN has a role in regulating mitotic control. To examine this possibility, *Pten*$^{+/+}$ and *Pten*$^{-/-}$ cells were treated with Taxol (100 nM), a drug that leads to mitotic arrest. Live cell-imaging time lapse experiments were performed to determine the time spent in mitosis (Fig. 7A). *Pten*$^{-/-}$ cells treated with taxol stayed in mitotic phase for less time (~50% or shorter) than *Pten*$^{+/+}$ cells, suggesting that *Pten*$^{-/-}$ cells bypass the mitotic checkpoint (Fig. 7A and B).

As a complementary approach, PTEN siRNA was used to deplete PTEN in HeLa cells (Fig. 5A). We treated control and PTEN-depleted cells with 100 nM Taxol to arrest cells in mitosis. Control cells exhibited a strong H3S10P signal after 24 hrs of Taxol treatment, indicating efficient arrest (Fig. 7C). The histone H3 serine 10P (H3S10P) signal decreased significantly after 36 hr of Taxol treatment, indicating that the HeLa cells eventually bypassed the mitotic checkpoint. In contrast, PTEN-depleted cells

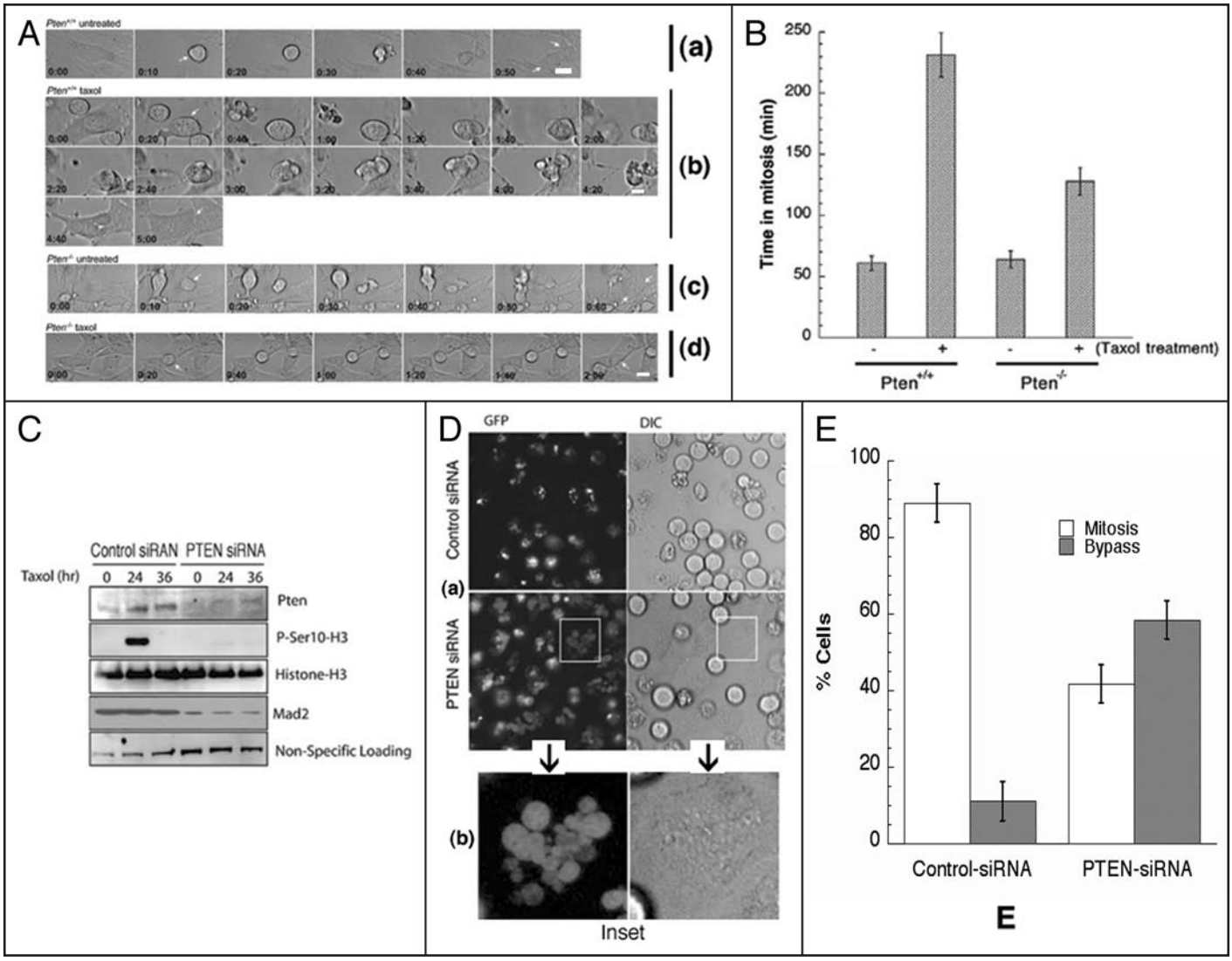


Figure 7. Response of Taxol treatment in cells with and without PTEN. (A) Asynchronous *Pten*$^{+/+}$ and *Pten*$^{-/-}$ MEFs were left untreated or treated with 100 nM taxol and analysed by live cell imaging. Examples of representative cells are shown. Arrows indicate the cells being followed. Where there are two arrows in the same plane this indicates that the cells have successfully divided. Scale bar represents 25 μm. (B) Histogram showing the effect of Taxol on the time in mitosis in cells with and without PTEN. (C) Effect of Taxol on phosphorylation of histone H3 at Ser 10 in HeLa cells with and without knockdown of PTEN. (D) HeLa cell-line stably expressing a GFP-tagged-histone H2B (GFP-H2B), transfected with control or PTEN specific siRNA were synchronized at the $G_1$/S boundary using double thymidine block and 4 hr following release from the block, taxol was added, and immunofluorescence images were acquired every 10 min for 16 hr and analysed for the percentage of cells that remained arrested in mitosis compared with cells that had bypassed mitotic arrest and become micronucleated with interphase morphology. Magnified inset shown as (Parts a and b). (E) Histogram showing percent of cells in mitosis and bypass checkpoint after PTEN knockdown and treatment with taxol.

displayed significantly reduced levels of H3S10P at 24 hrs of Taxol treatment, suggesting that the cells bypassed the mitotic checkpoints more quickly than drug treated control siRNA transfected cells (Fig. 7C and E). PTEN depletion did not affect overall levels of H3 protein itself (Fig. 7C).

To more thoroughly characterize the response of PTEN-deficient cells to taxol, we employed a HeLa cell-line stably expressing GFP-tagged-histone H2B (GFP-H2B), a line commonly used for analysis of mitotic progression. GFP-H2B-HeLa cells transfected with control or PTEN specific siRNA were synchronized at the $G_1$/S boundary using a double thymidine block. Four hours after release from the block, taxol was added, and immunofluorescence images were acquired every 10 min for 16 hr to determine the percentage of cells that remained arrested in mitosis or bypassed the mitotic arrest to become micronucleated with interphase morphology (Fig. 7D). We considered cells that contained numerous micronuclei and a flattened morphology to have undergone mitotic bypass (Fig. 7D and Inset a and d). While the majority of control siRNA transfected cells (>90%) remained arrested in mitosis after 16 hrs in Taxol, a significantly increased proportion of PTEN depleted cells exhibited mitosis bypass (Fig. 7E).

To further our understanding of where PTEN functions in the spindle assembly checkpoint pathway we analyzed Mad2 protein expression, which ensures proper checkpoint execution by

localizing to unattached, but not attached, kinetochores to prevent anaphase promoting complex activity. Notably, we observed a modest reduction in the level of Mad2 protein expression in PTEN-depleted human cells or *Pten*$^{-/-}$ mouse embryonic fibroblasts (Fig. 7C and data not shown).

## Discussion

DNA damage repair and checkpoint control are the two major mechanisms that function to maintain genomic stability. Checkpoints regulate cell cycle progression post DNA damage and during replication to ensure sufficient time for DNA repair. Defects in cell cycle progression can occur at multiple points and lead to cells with a high frequency of structural as well as numerical chromosomal aberrations. A similar increase in structural as well as numerical chromosome aberrations has been observed in cells with reduced levels of PTEN. In this study, we provide direct evidence that genomic instability in PTEN deficient cells, both the structural as well as numerical chromosome aberrations, is not due to defective DNA DSB repair pathways but rather multiple defective checkpoints.

DNA damage response checkpoints have been identified at the $G_1$/S and $G_2$/M boundaries during S-phase and in mitosis.[41] Cells initiate DNA damage checkpoints after replication or cell stress to provide sufficient time for the repair of DNA damage. Specifically, intra-S checkpoints prevent cells from unfaithful genome replication, the $G_2$/M checkpoint is initiated to allow for repair of DNA damage prior to mitosis and the mitotic checkpoints guarantee faithful segregation of chromosomes. Since DNA repair and checkpoint induction are closely interlinked, some gene products may function in both processes while others may be restricted to either DNA repair or checkpoint functions.[37,42-46]

Loss of PTEN does not alter ATM activation and, since ATM is upstream of activators of damage inducible checkpoint arrest,[47] this suggests that damage induced ATM effector functions are independent of PTEN. This is further supported by the fact that ATM dependent phosphorylation of KAP1, H2AX, Chk2, SMC1, which are involved in the process of DNA damage sensing and repair, is also independent of PTEN function. Specifically, KAP1 is involved in post irradiation chromatin alterations that provide repair proteins access to the damaged DNA.[23] Since KAP1 functions independent of PTEN status, PTEN deficient cells do not have an altered chromatin structures that could hamper DNA repair. In addition, stress like heat shock has been reported to influence chromatin structure. Interestingly, cells with and without PTEN showed a similar response to the induction of HSP70 (Suppl. Fig. 1) as well as KAP1 phosphorylation, arguing against a role for PTEN in chromatin modification after stress or DNA damage.

Several reports have indicated that reduced levels of PTEN are associated with radioresistance, which can be suppressed by ectopic PTEN expression.[48,49] This recovery of radiation sensitivity was attributed to the ability of PTEN to suppress DNA repair capacity.[50] In contrast, Shen and coworkers reported that PTEN is important for DNA DSB repair by regulating Rad51 expression[4] and that PTEN influences γ-H2AX as well as 53BP1 foci formation, suggesting that PTEN is involved in NHEJ as well as HR mediated repair. However, perusal of the literature reveals that cells defective in NHEJ and HR are usually highly sensitive, not resistant, to IR-induced cell killing.

Ionizing radiation induced γ-H2AX foci are a surrogate marker for DNA DSBs, however a systematically analysis of IR-induced γ-H2AX foci appearance and disappearance in cells with and without PTEN indicated no differences (Fig. 1C–E). The 53BP1 DNA damage response protein also did not show any difference in IR-induced foci formation between cells with and without PTEN. Likewise loss of PTEN had no effect on Rad51 protein levels or IR-induced Rad51 foci formation, the key feature of DNA strand invasion during homologous recombination (Fig. 1F). Thus the initial steps of DNA damage sensing and chromatin modification associated with DNA DSBs are similar in cells with and without PTEN, suggesting defective repair is not the cause for the higher genomic instability observed in PTEN deficient cells.

DNA double-strand breaks lead to chromosomal structural alterations if not repaired in an accurate and timely manner. However, neither the induction of DNA DSBs post irradiation, the kinetics of DNA DSB repair nor the level of residual DNA damage (90 min or 120 min of post irradiation) was altered by the loss of PTEN (Fig. 5). Furthermore, cell cycle phase specific DNA DSB repair was identical between cells with and without PTEN (Fig. 5). Such results further argue against a role for PTEN in DNA DSB repair.



Loss of PTEN function, either by mutation or epigenetic modification, results in constitutive activation of Akt and its downstream substrates.[51,52] Since the PTEN-PI3K-Akt pathway has become a critical target for inhibition in cancer therapeutics, it is important to understand the basis of genomic instability in cells deficient for PTEN as these cells are modestly resistant to DNA damaging agents like IR. Examination of multiple PTEN deficient cell lines did not identify any displaying loss of Rad51, whereas all such cell lines contained the phosphorylated form of AKT (Fig. 2A and Suppl. Fig. 2D), which is consistent with the PTEN function, that cells overexpressing PTEN are radiosensitive.[50,53] Biochemical assays also revealed that PTEN deficiency neither abrogates DDR nor the DNA ligation process. In a comparison of IR-induced chromosome aberrations at different stages of the cell cycle, PTEN deficient cells were found to have increased S- and $G_2$-phase specific chromosome aberrations. Repair by HR predominates in cells in these cell cycle phases due to the presence of sister chromatids that function as templates for repair. However, PTEN deficient cells did not show any deficiency in IR induced Rad51 foci formation nor a reduced frequency of HR dependent I-Sec1 induced DSB repair as pDR-GFP cells treated with PTEN siRNA had no reduction in the number of GFP positive cells in comparison to control transfected cells. This provides strong evidence that PTEN deficiency does not affect the HR pathway for DNA DSB repair. Furthermore PTEN deficient cells have a similar frequency of sister chromatid exchanges as well as telomere recombination as observed in cells with PTEN, also suggesting that HR is intact in PTEN deficient cells.

PTEN, with a lipid-binding domain and the absence of a canonical nuclear localization signal, was first reported as

exclusively in the cytoplasm.[54-56] However nuclear PTEN was noted in neuronal and breast tissues or cell lines and in primary, differentiated and resting cells, compared to rapidly cycling cancer cell lines where in many cases there is a marked reduction of nuclear PTEN.[57-59] Interestingly PTEN has been identified in punctate forms near or on the centromeres, supporting the argument that the absence of PTEN results in centromere breakage.[4] It is possible that PTEN may be involved in the dephosphorylation of enzymes required for centromeric DNA separation. In this case its absence may result in either breakage in the centromere and surrounding regions or complete failure of separation of chromatid centromeres, producing butterfly types of chromosome morphology. In contrast we found that cells deficient in PTEN do have frequent chromosome fragments with and without centromere, but also chromosomes fragments with multiple centromere and no butterfly type of chromosome morphology, which does not fit with the supposed function of PTEN on centromeres. If PTEN is a centromere binding protein or has a role during DNA synthesis, it should be constitutively present in the nucleus of dividing cells. However, the situation is different based on the perusal of literature as well as our present study in that PTEN does not show any interaction with the centromeric DNA or genomic DNA (Fig. 4). Besides PTEN deficient cells do a have high frequency of polyploidy with intact centromeric structure, ruling out the possibility of PTEN's role in centromeric function (Suppl. Fig. 6).

The presence of chromosome fragments with multiple centromeres (Fig. 3A) is suggestive of abnormal DNA synthesis, possibly due to defective S-phase checkpoints. A higher frequency of chromosomal aberrations at metaphase can be due to multiple defective cell cycle checkpoints. The present studies revealed that PTEN deficient cells have an intact DNA damage induced $G_1$ checkpoint as evidenced by the fact that cells treated with caffeine and then irradiated in $G_1$ had increased chromosome aberrations as compared to cells irradiated without drug irrespective of PTEN status (Fig. 6). However, in caffeine or KU-55933 treated cells irradiated in S- and/or $G_2$-phase, an increased frequency of chromosomal aberrations was observed only in cells with PTEN, and not in cells lacking PTEN (Fig. 6 and data not shown), supporting the argument that PTEN deficient cells lack S- or $G_2$-phase checkpoints, an observation consistent with our previous results.[3] In addition, PTEN deficient cells have a higher mitotic index post irradiation as compared to cells with PTEN, suggesting that PTEN deficient cells also have a defective $G_2$/M checkpoint. This was further confirmed by the fact that when cells were challenged with Taxol and monitored by live cell imaging for the time required to complete mitosis, PTEN deficient cells bypassed the spindle assembly checkpoint quickly as compared to cells with PTEN (Figs. 6D and 7). This accelerated checkpoint bypass alone can account for the aneuploidy as well the polyploidy observed in PTEN deficient cells, since there was no evidence that PTEN interacts with centromeric DNA that could hamper the segregation of the chromosomes. The goal now is to provide mechanistic insights into the role of PTEN in regulation of spindle assembly checkpoint, a well characterized pathway to genomic instability.

## Material and Methods

**Cells.** Mouse embryonic fibroblasts (MEFs) and embryonic stem (ES) cells with and without PTEN were cultured as described previously,[2-5] mouse kidney fibroblasts with and without ATM (*Atm*$^{+/+}$ and *Atm*$^{-/-}$), and MCF7 cells were maintained following published procedures.[5,6] DLD1PTEN$^{+/+}$, DLD1PTEN$^{-/-}$, HCT116PTEN$^{+/+}$, HCT116PTEN$^{-/-}$, TIG-1, WI38, HeLa and U2OS cells were grown at 37°C in a 5% $CO_2$ incubator in low glucose DMEM supplemented with 10% FCS, 50 U/ml penicillin and 5 mg/ml streptomycin. For oxidative stress, cells were treated with $H_2O_2$ (150 μM for 2 h). Cells were irradiated with gamma rays at the rate of 1 Gy per minute. Heat shock treatments were carried out at 43°C for 30 min and allowed to recover at 37°C for increasing intervals.

**Antibodies and siRNA.** ATM, phospho-ATM Ser1981, H2AX, phosphorylated H2AX, 53BP1, Chk1, phosphorylated Chk1, are the same described previously[5,7,8] Rad51 from different sources (Santa Cruz, Oncogene) Abcam; KAP-1 and Phosphospecific KAP-1 form Bethyl Laboratories, TX; from Abcam; PTEN from Cell Signaling Technology, Incorporation, and gift form Dr. Yuxin Yin and CENP-C from Santa Cruz. Small interfering RNA (siRNA) for specific gene and control Luc siRNA were obtained from Dharmacon Research (Lafayette, CO and Santa Cruz).



**Western blot analysis and immunoprecipitation.** Cell lysate preparations, immunoblotting and detection of specific proteins were done according to previously described procedures.[7,8] For immunoprecipitation, cells were lysed in lysis buffer and precleaned with protein A/G beads. Proteins were immunoprecipitated with specific antibodies and immunoprecipitants were washed with lysis buffer as previously described.[7,8]

**Chromatin immunoprecipitation.** Coimmunoprecipitation after formaldehyde-mediated in vivo cross-linking of DNA with proteins was performed with a different antibody as described previously.[9,10] Immunoprecipitated DNA was spotted onto a membrane by using a dot blotting apparatus and then hybridized to $^{32}$P-labeled DNA probes. The probes used for hybridization were telomeric repeat DNA, centromeric repeat DNA, and total human. The blots were stripped and successively hybridized with different probes.

**Immunofluorescence measurements of damage induced foci.** Cell culture in chamber slides, fixation and immunostaining were done as previously described.[5,11-13] Fluorescent images of foci were captured with a Zeiss Axioskop 2 mot epifluorescent microscope equipped with a charge-coupled device camera and ISIS software (Metasystems, Altlussheim, Germany). Optical sections through nuclei were captured and the images were obtained by projection of the individual sections as recently described.[14] The results shown are from three independent experiments. Cells with bubble-like appearance or micronuclei were not considered for γ-H2AX analysis.

**DNA DSB analysis.** Two different assays were used to measure DNA strand breaks after IR exposure. These were (a) pulsed field

gel electrophoresis (PFGE) and (b) neutral filter elution. In the PFGE, cells were irradiated, embedded in agarose plugs, and lysed in situ. Plugs were washed in Tris-EDTA buffer [10 mmol/L Tris-HCl, 1 mmol/L $Na_2EDTA$ (pH 8)] and PFGE was carried out as described recently.[12] Subsequently, gels were ethidium bromide stained and photographed with a charge-coupled device camera system under UV transillumination. Quantitative analysis to determine the fraction of DNA entering the gel provided a measure for the relative number of double-strand breaks. The control cell DNA was normalized to zero and a relative value of 1 was assigned to DNA of cells treated with 20 Gy.

The level of DNA DSBs in cells were also estimated by neutral filter elution as described previously.[15] Cells were labeled for a period of one-and-one-half doublings and then were washed free of radioactive medium and reincubated in nonradioactive medium for an additional 3 h prior to the experiment. Cells were exposed to IR and incubated at 37°C for different times postirradiation. Cells were layered onto polycarbonated filters, lysed and eluted under neutral conditions (pH 9.6) as described previously.[15] Relative elution (RE) was calculated as RE % & log(FI/Fc), where FI and Fc are the fractions of DNA left on the filter for the irradiated (I) and unirradiated (c) cells when 75% of the internal standard DNA is left on the filter.

Cell-based analysis of individual chromosome damage at metaphase provides the most sensitive assay for determining the DNA damage. Metaphase chromosome spreads were prepared by procedures described earlier.[16] Giemsa-stained chromosomes of metaphase spreads were analyzed for chromosome aberrations. $G_1$-type chromosomal aberrations were assessed as described previously.[17] The categories of $G_1$-type asymmetrical chromosome aberrations scored included dicentrics, centric rings, interstitial deletions and acentric rings, and terminal deletions. S-phase-specific chromosomal aberrations were analyzed at metaphase. Exponentially growing cells were irradiated with 2 Gy, and mitotic cells were collected 3 to 4 h postirradiation. Both chromosome and chromatid aberrations were scored. For $G_2$-specific chromosomal aberrations, cells in exponential phase were irradiated with 1 Gy and metaphases were collected at 45 and 90 min following irradiation and examined for chromatid breaks and gaps per metaphase as described previously.[5,18] To determine whether PTEN inactivation influences chromosome repair, cells were treated with caffeine (2 mmol/L) 4 h before irradiation. The ATM inhibitor (ATMi) KU-55933 was from KuDos Pharmaceuticals and was used at a final concentration of 10 μM. Two hundred metaphases were analyzed for each point.

**Telomere length analysis.** To analyze telomere length, we performed Q-FISH and TRF analyses according to procedures described previously.[19]

**Detection of telomeric circles.** Genomic DNA were isolated and digested by standard protocols.[9,10] For standard telomere blots, digested genomic DNA was fractionated on a 0.7% agarose gel containing 0.1 μg/ml ethidium bromide (EtBr) in 1x TAE at ~2 V/cm overnight. Neutral-neutral 2D gel electrophoresis was performed according to the established protocols[20] with the modifications as described previously.[21]

**Enrichment of cells population by centrifugal elutriation.** Exponentially growing cell populations (1.3–1.5 x $10^8$ cells) were resuspended in 50 ml of elutriation buffer [1x Hanks' balanced salt solution containing 3.3% heat-inactivated bovine calf serum and 5 mM 2-naphthol-6,8-disulfonic acid dipotassium salt (NDA), Eastman Kodak Company, Rochester, NY] pH 7. To this, 4 ml of 0.02% (w/v) of DNase I type IV (Sigma), dissolved in RPMI 1640 medium, was added. The cells were placed on ice, passed through a 23G needle and nylon mesh to remove cell aggregates, and then loaded into a Beckman elutriator rotor at 2,000 rpm at a pump rate of 13.5 ml/min at 4°C. Following a 100-ml buffer wash, 18 fractions were elutriated by step-wise increases in pump speed from 14 to 32 ml/min. After separation, the cell fractions were placed on ice to prevent cell cycle progression. The viability of the cells was not affected by elutriation as monitored by trypan blue exclusion. The cell cycle distributions of the fractionated samples were determined using flow cytometry to measure DNA content. Aliquots of each fraction were washed twice in phosphate-buffered saline (PBS), fixed in 70% ethanol: 30% PBS, incubated at 37°C with 0.5% RNAse, and stained with propidium iodide. DNA content was determined by quantitative flow cytometry using a FacScan analyzer. The accuracy of the analyzer was checked with calibrated fluorescent beads and chicken erythrocytes. The $G_1$-phase enriched populations contained more than 93% $G_1$-phase cells, the S-phase enriched population contained 85–89% S-phase cells and $G_2$/M phase enriched population contained 73–79% of $G_2$/M cells.

**Timelapse microscopy.** Live cell imaging of MEFs was conducted using an Olympus IX81 microscope with 40x magnification lens. Cells were treated with 100 nM taxol. Images were taken every 10 min. Image analysis was done using the analySIS LS Research version 2.2. Live cell imaging of HeLa H2B cells was done using a Deltavision Core microscope with 40x magnification lens. Cells were synchronized by double thymidine block. Images were analyzed using softWoRx version 3.6.1.



**Acknowledgements**

This work was supported by National Institute of Health grants CA129537 and CA123232 (T.K.P.). We thank Shyam K. Sharan, Yuxin Yin, Titia DeLange, Susana Gonzalo, Todd Waldman, T. Halazonetis and C. Eng for providing the reagents, sharing data and advice. We thank the members of Pandita laboratory for their help and thoughtful discussion.

**Note**

Supplementary materials can be found at:
www.landesbioscience.com/supplement/GuptaCC8-14-Sup.pdf

**References**

1. Stambolic V, Suzuki A, de la Pompa JL, Brothers GM, Mirtsos C, Sasaki T, et al. Negative regulation of PKB/Akt-dependent cell survival by the tumor suppressor PTEN. Cell 1998; 95:29-39.
2. Sun H, Lesche R, Li DM, Liliental J, Zhang H, Gao J, et al. PTEN modulates cell cycle progression and cell survival by regulating phosphatidylinositol 3,4,5,-trisphosphate and Akt/protein kinase B signaling pathway. Proc Natl Acad Sci USA 1999; 96:6199-204.
3. Puc J, Keniry M, Li HS, Pandita TK, Choudhury AD, Memeo L, et al. Lack of PTEN sequesters CHK1 and initiates genetic instability. Cancer Cell 2005; 7:193-204.
4. Shen WH, Balajee AS, Wang J, Wu H, Eng C, Pandolfi PP, et al. Essential role for nuclear PTEN in maintaining chromosomal integrity. Cell 2007; 128:157-70.

5. Pandita RK, Sharma GG, Laszlo A, Hopkins KM, Davey S, Chakhparonian M, et al. Mammalian rad9 plays a role in telomere stability, s- and g2-phase-specific cell survival, and homologous recombinational repair. Mol Cell Biol 2006; 26:1850-64.
6. Hunt CR, Dix DJ, Sharma GG, Pandita RK, Gupta A, Funk M, et al. Genomic instability and enhanced radiosensitivity in Hsp70.1- and Hsp70.3-deficient mice. Mol Cell Biol 2004; 24:899-911.
7. Gupta A, Sharma GG, Young CS, Agarwal M, Smith ER, Paull TT, et al. Involvement of human MOF in ATM function. Mol Cell Biol 2005; 25:5292-305.
8. Pandita TK, Lieberman HB, Lim DS, Dhar S, Zheng W, Taya Y, et al. Ionizing radiation activates the ATM kinase throughout the cell cycle. Oncogene 2000; 19:1386-91.
9. Sharma GG, Gupta A, Wang H, Scherthan H, Dhar S, Gandhi V, et al. hTERT associates with human telomeres and enhances genomic stability and DNA repair. Oncogene 2003; 22:131-46.
10. Sharma GG, Hwang KK, Pandita RK, Gupta A, Dhar S, Parenteau J, et al. Human heterochromatin protein 1 isoforms HP1(Hsalpha) and HP1(Hsbeta) interfere with hTERT-telomere interactions and correlate with changes in cell growth and response to ionizing radiation. Mol Cell Biol 2003; 23:8363-76.
11. Pandita TK, Westphal CH, Anger M, Sawant SG, Geard CR, Pandita RK, et al. Atm inactivation results in aberrant telomere clustering during meiotic prophase. Mol Cell Biol 1999; 19:5096-105.
12. Hunt CR, Pandita RK, Laszlo A, Higashikubo R, Agarwal M, Kitamura T, et al. Hyperthermia activates a subset of ataxia-telangiectasia mutated effectors independent of DNA strand breaks and heat shock protein 70 status. Cancer Res 2007; 67:3010-7.
13. Agarwal M, Pandita S, Hunt CR, Gupta A, Yue X, Khan S, et al. Inhibition of telomerase activity enhances hyperthermia-mediated radiosensitization. Cancer Res 2008; 68:3370-8.
14. Scherthan H, Jerratsch M, Dhar S, Wang YA, Goff SP, Pandita TK. Meiotic telomere distribution and Sertoli cell nuclear architecture are altered in Atm- and Atm-p53-deficient mice. Mol Cell Biol 2000; 20:7773-83.
15. Pandita TK, Hittelman WN. Initial chromosome damage but not DNA damage is greater in ataxia telangiectasia cells. Radiat Res 1992; 130:94-103.
16. Pandita TK. Effect of temperature variation on sister chromatid exchange frequency in cultured human lymphocytes. Hum Genet 1983; 63:189-90.
17. Pandita TK, Geard CR. Chromosome aberrations in human fibroblasts induced by monoenergetic neutrons I. Relative biological effectiveness. Radiat Res 1996; 145:730-9.
18. Dhar S, Squire JA, Hande MP, Wellinger RJ, Pandita TK. Inactivation of 14-3-3sigma influences telomere behavior and ionizing radiation-induced chromosomal instability. Mol Cell Biol 2000; 20:7764-72.
19. Gonzalo S, Jaco I, Fraga MF, Chen T, Li E, Esteller M, et al. DNA methyltransferases control telomere length and telomere recombination in mammalian cells. Nat Cell Biol 2006; 8:416-24.
20. Brewer BJ, Fangman WL. The localization of replication origins on ARS plasmids in *S. cerevisiae*. Cell 1987; 51:463-71.
21. Cohen S, Lavi S. Induction of circles of heterogeneous sizes in carcinogen-treated cells: two-dimensional gel analysis of circular DNA molecules. Mol Cell Biol 1996; 16:2002-14.
22. Bakkenist CJ, Kastan MB. DNA damage activates ATM through intermolecular autophosphorylation and dimer dissociation. Nature 2003; 421:499-506.
23. Ziv Y, Bielopolski D, Galanty Y, Lukas C, Taya Y, Schultz DC, et al. Chromatin relaxation in response to DNA double-strand breaks is modulated by a novel ATM- and KAP-1 dependent pathway. Nat Cell Biol 2006; 8:870-6.
24. Fernandez-Capetillo O, Celeste A, Nussenzweig A. Focusing on foci: H2AX and the recruitment of DNA-damage response factors. Cell Cycle 2003; 2:426-7.
25. Pilch DR, Sedelnikova OA, Redon C, Celeste A, Nussenzweig A, Bonner WM. Characteristics of gamma-H2AX foci at DNA double-strand breaks sites. Biochem Cell Biol 2003; 81:123-9.
26. Riballo E, Kuhne M, Rief N, Doherty A, Smith GC, Recio MJ, et al. A pathway of double-strand break rejoining dependent upon ATM, Artemis and proteins locating to gamma-H2AX foci. Mol Cell 2004; 16:715-24.
27. Rogakou EP, Pilch DR, Orr AH, Ivanova VS, Bonner WM. DNA double-stranded breaks induce histone H2AX phosphorylation on serine 139. J Biol Chem 1998; 273:5858-68.
28. Ward IM, Chen J. Histone H2AX is phosphorylated in an ATR-dependent manner in response to replicational stress. J Biol Chem 2001; 276:47759-62.
29. Petersen S, Casellas R, Reina-San-Martin B, Chen HT, Difilippantonio MJ, Wilson PC, et al. AID is required to initiate Nbs1/gamma-H2AX focus formation and mutations at sites of class switching. Nature 2001; 414:660-5.
30. Mahadevaiah SK, Turner JM, Baudat F, Rogakou EP, de Boer P, Blanco-Rodriguez J, et al. Recombinational DNA double-strand breaks in mice precede synapsis. Nat Genet 2001; 27:271-6.
31. Chen HT, Bhandoola A, Difilippantonio MJ, Zhu J, Brown MJ, Tai X, et al. Response to RAG-mediated VDJ cleavage by NBS1 and gamma-H2AX. Science 2000; 290:1962-5.
32. Bassing CH, Chua KF, Sekiguchi J, Suh H, Whitlow SR, Fleming JC, et al. Increased ionizing radiation sensitivity and genomic instability in the absence of histone H2AX. Proc Natl Acad Sci USA 2002; 99:8173-8.
33. Bassing CH, Swat W, Alt FW. The mechanism and regulation of chromosomal V(D)J recombination. Cell 2002; 109:45-55.
34. Mochan TA, Venere M, DiTullio RA Jr, Halazonetis TD. 53BP1, an activator of ATM in response to DNA damage. DNA Repair (Amst) 2004; 3:945-52.
35. Pandita TK, DeRubeis D. Spontaneous amplification of interstitial telomeric bands in Chinese hamster ovary cells. Cytogenet Cell Genet 1995; 68:95-101.
36. Pandita TK, Hittelman WN. The contribution of DNA and chromosome repair deficiencies to the radiosensitivity of ataxia-telangiectasia. Radiat Res 1992; 131:214-23.
37. Scott SP, Pandita TK. The cellular control of DNA double-strand breaks. J Cell Biochem 2006.
38. Radford IR. The level of induced DNA double-strand breakage correlates with cell killing after X-irradiation. Int J Radiat Biol Relat Stud Phys Chem Med 1985; 48:45-54.
39. Radford IR. Evidence for a general relationship between the induced level of DNA double-strand breakage and cell-killing after X-irradiation of mammalian cells. Int J Radiat Biol Relat Stud Phys Chem Med 1986; 49:611-20.
40. Weaver BA, Cleveland DW. Does aneuploidy cause cancer? Curr Opin Cell Biol 2006; 18:658-67.
41. Lukas J, Lukas C, Bartek J. Mammalian cell cycle checkpoints: signalling pathways and their organization in space and time. DNA Repair (Amst) 2004; 3:997-1007.
42. Zhou BB, Elledge SJ. The DNA damage response: putting checkpoints in perspective. Nature 2000; 408:433-9.
43. van Gent DC, Hoeijmakers JH, Kanaar R. Chromosomal stability and the DNA double-stranded break connection. Nat Rev Genet 2001; 2:196-206.
44. Wahl GM, Carr AM. The evolution of diverse biological responses to DNA damage: insights from yeast and p53. Nat Cell Biol 2001; 3:277-86.
45. Jeggo PA, Lobrich M. Contribution of DNA repair and cell cycle checkpoint arrest to the maintenance of genomic stability. DNA Repair (Amst) 2006; 5:1192-8.
46. Shiloh Y. ATM and related protein kinases: safeguarding genome integrity. Nat Rev Cancer 2003; 3:155-68.
47. Lavin MF, Khanna KK. ATM: the protein encoded by the gene mutated in the radiosensitive syndrome ataxia-telangiectasia. Int J Radiat Biol 1999; 75:1201-14.
48. Wick W, Furnari FB, Naumann U, Cavenee WK, Weller M. PTEN gene transfer in human malignant glioma: sensitization to irradiation and CD95L-induced apoptosis. Oncogene 1999; 18:3936-43.
49. Rosser CJ, Tanaka M, Pisters LL, Tanaka N, Levy LB, Hoover DC, et al. Adenoviral-mediated PTEN transgene expression sensitizes Bcl-2-expressing prostate cancer cells to radiation. Cancer Gene Ther 2004; 11:273-9.
50. Pappas G, Zumstein LA, Munshi A, Hobbs M, Meyn RE. Adenoviral-mediated PTEN expression radiosensitizes non-small cell lung cancer cells by suppressing DNA repair capacity. Cancer Gene Ther 2007; 14:543-9.
51. Yilmaz OH, Valdez R, Theisen BK, Guo W, Ferguson DO, Wu H, et al. Pten dependence distinguishes haematopoietic stem cells from leukaemia-initiating cells. Nature 2006; 441:475-82.
52. Cantley LC, Neel BG. New insights into tumor suppression: PTEN suppresses tumor formation by restraining the phosphoinositide 3-kinase/AKT pathway. Proc Natl Acad Sci USA 1999; 96:4240-5.
53. Kao GD, Jiang Z, Fernandes AM, Gupta AK, Maity A. Inhibition of phosphatidylinositol-3-OH kinase/Akt signaling impairs DNA repair in glioblastoma cells following ionizing radiation. J Biol Chem 2007; 282:21206-12.
54. Lee JO, Yang H, Georgescu MM, Di Cristofano A, Maehama T, Shi Y, et al. Crystal structure of the PTEN tumor suppressor: implications for its phosphoinositide phosphatase activity and membrane association. Cell 1999; 99:323-34.
55. Li DM, Sun H. TEP1, encoded by a candidate tumor suppressor locus, is a novel protein tyrosine phosphatase regulated by transforming growth factor beta. Cancer Res 1997; 57:2124-9.
56. Whang YE, Wu X, Suzuki H, Reiter RE, Tran C, Vessella RL, et al. Inactivation of the tumor suppressor PTEN/MMAC1 in advanced human prostate cancer through loss of expression. Proc Natl Acad Sci USA 1998; 95:5246-50.
57. Lachyankar MB, Sultana N, Schonhoff CM, Mitra P, Poluha W, Lambert S, et al. A role for nuclear PTEN in neuronal differentiation. J Neurosci 2000; 20:1404-13.
58. Sano T, Lin H, Chen X, Langford LA, Koul D, Bondy ML, et al. Differential expression of MMAC/PTEN in glioblastoma multiforme: relationship to localization and prognosis. Cancer Res 1999; 59:1820-4.
59. Salmena L, Carracedo A, Pandolfi PP. Tenets of PTEN tumor suppression. Cell 2008; 133:403-14.